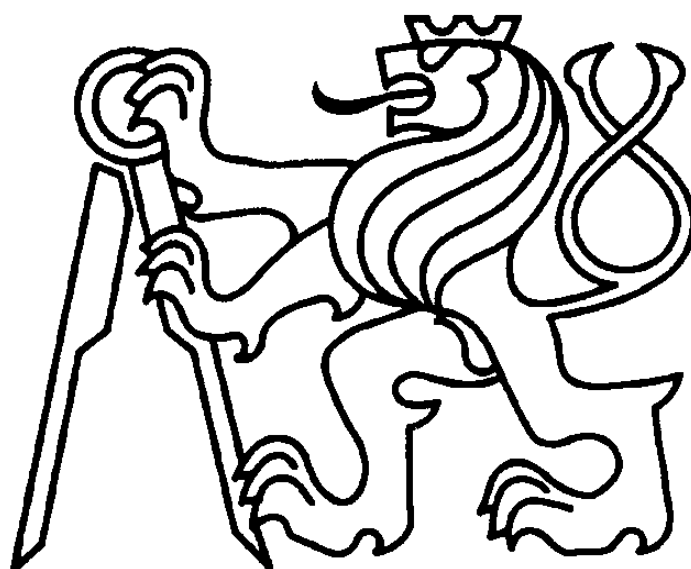


CZECH TECHNICAL UNIVERSITY IN PRAGUE

FACULTY OF ELECTRICAL ENGINEERING



BACHELOR'S THESIS

**Stimulus-frequency otoacoustic emissions
measured using synchronized swept sines**

Author: Yiming Peng

Thesis supervisor: Ing. Václav Vencovský, Ph.D.

Department of Radio Electronics

January 2024



BACHELOR'S THESIS ASSIGNMENT

I. Personal and study details

Student's name: **Peng Yiming** Personal ID number: **498587**
Faculty / Institute: **Faculty of Electrical Engineering**
Department / Institute: **Department of Electrical Power Engineering**
Study program: **Electrical Engineering and Computer Science**

II. Bachelor's thesis details

Bachelor's thesis title in English:

Stimulus-frequency otoacoustic emissions measured using synchronized swept sines.

Bachelor's thesis title in Czech:

Měření otoakustických emisí evokovaných jedním tónem pomocí rozmitaného tónu.

Guidelines:

Implement an approach for measuring stimulus-frequency otoacoustic emissions (SFOAEs) by using synchronized swept sines. SFOAEs have the same frequency as the evoking stimulus. Therefore, compression or suppression methods are used to extract the emissions. Focus on the possibility of using the suppression method together with the synchronized swept-sine technique. Verify the developed approach experimentally using SFOAEs measured in human ears.

Bibliography / sources:

[1] Novak A, Simon L, Lotton P. Synchronized Swept-Sine: Theory, Application, and Implementation. J Audio Eng Soc, 2015, 63 (10), 786-798. <https://doi.org/10.17743/jaes.2015.0071>
[2] Charaziak KK, Shera CA. Reflection-Source Emissions Evoked with Clicks and Frequency Sweeps: Comparisons Across Levels. J Assoc Res Otolaryngol. 2021;22(6):641-658. doi: 10.1007/s10162-021-00813-3.

Name and workplace of bachelor's thesis supervisor:

Ing. Václav Vencovský, Ph.D. Department of Radioelectronics FEE

Name and workplace of second bachelor's thesis supervisor or consultant:

Date of bachelor's thesis assignment: **15.09.2023** Deadline for bachelor thesis submission: **09.01.2024**

Assignment valid until: **16.02.2025**

Ing. Václav Vencovský, Ph.D.
Supervisor's signature

doc. Ing. Zdeněk Müller, Ph.D.
Head of department's signature

prof. Mgr. Petr Páta, Ph.D.
Dean's signature

III. Assignment receipt

The student acknowledges that the bachelor's thesis is an individual work. The student must produce his thesis without the assistance of others, with the exception of provided consultations. Within the bachelor's thesis, the author must state the names of consultants and include a list of references.

Date of assignment receipt

Student's signature

Declaration

I hereby declare that this bachelor's thesis is the product of my own independent work and that I have clearly stated all information sources used in the thesis according to Methodological Instruction No. 1/2009 – “On maintaining ethical principles when working on a university final project, CTU in Prague”.

Date:

Signature:

Acknowledgement

I would like to express my thanks to my colleagues and teachers at the Department of Radio electronics of the Faculty of Electrical Engineering of Czech Technical University in Prague for their wide support. Especially thanks to my supervisor Ing. Václav Vencovský, Ph.D., I can't complete my project and bachelor's thesis without his patiently guide and help. Special thanks belong to my roommates and parents for tolerance and patience.

Abstract

This research investigates the feasibility of measuring Stimulus-Frequency Otoacoustic Emissions (SFOAEs) using synchronized swept sines. SFOAEs are acoustical signals generated from within the inner ear (cochlea) in response to stimulation with a single pure tone. In this study, we investigate the efficacy of integrating the suppression method with the synchronized swept sine technique for the extraction of SFOAEs. A critical aspect in this approach is the potential interaction of the suppressor-induced impulse response with the impulse response which contains the SFOAE signal. This interaction poses a risk of distortion, as the suppressor response may closely align with the SFOAE response. Our thesis primarily focuses on examining and quantifying the extent of this potential distortion for various stimulus intensities and sweep rates. The utilization of swept sine in the extraction of SFOAEs presents significant advantages: high frequency resolution and rapid extraction of SFOAEs allowing its visualization during measurement. In the conclusion of this thesis, we could say that we can use the SSS technique for SFOAEs extracted using suppression method.

Key words: Stimulus-frequency Otoacoustic Emissions, synchronized swept sines, suppression, SFOAEs extraction, signal analysis.

Abstrakt

Tato bakalářská práce zkoumá proveditelnost měření otoakustických emisí evokovaných jedním tónem (SFOAE) pomocí synchronizovaných rozmítaných tónů. SFOAE jsou akustické signály generované z vnitřního ucha (kochley) v reakci na stimulaci jediným čistým tónem. V této práci zkoumáme možnost použití metody extrakce SFOAE evokovaných rozmítanými siny při současném použití dodatečného tónu (supresoru). Konkrétně se musíme zaměřit na potenciální interakci supresorem indukované impulzní odezvy s impulzní odezvou, která obsahuje signál SFOAE. Tato interakce představuje riziko zkreslení měřeného SFOAE. Naše práce se primárně zaměřuje na zkoumání a kvantifikaci rozsahu tohoto potenciálního zkreslení s cílem zpřesnit proces extrakce SFOAE pomocí techniky synchronizovaného rozmítaného tónu pro různé intenzity stimulů a rychlosti rozmítání. Využití rozmítaného tónu při extrakci SFOAE představuje významné výhody: vysoké frekvenční rozlišení a nízká výpočtní náročnost extrakce umožňuje vizualizovat výsledek během měření. V závěru této práce bychom mohli říci, že pro SFOAE extrahované pomocí supresní metody můžeme použít techniku SSS.

Klíčová slova: Stimulační frekvenční otoakustické emise, synchronizované rozmítané tóny, potlačení, extrakce SFOAEs, analýza signálu.

List of content

LIST OF FIGURES.....	7
LIST OF TABLES.....	8
LIST OF ABBREVIATIONS.....	9
1. INTRODUCTION	10
1.1 ORGANIZATION OF THE THESIS.....	10
2. STIMULUS FREQUENCY OTOACOUSTIC EMISSIONS.....	11
2.1 COMPRESSION, SUPPRESSION AND SPECTRAL SMOOTHING	12
3. SYNCHRONIZED SWEEPED SINE FOR SFOAE MEASUREMENT.....	14
4. METHODS	18
4.1. SUBJECT.....	18
4.2. STIMULI.....	19
4.3. DATA ACQUISITION.....	21
4.4. NF (NOISE FLOOR) PROCESSING	25
5. RESULTS	25
5.1 EFFECT OF STIMULUS INTENSITY ON SFOAES EXTRACTED BY SSS	26
5.2 EFFECT OF SWEEP RATE ON SFOAES EXTRACTED BY SSS	32
6. CONCLUSION.....	35
7. REFERENCES.....	36

List of figures

Figure. 1. Two components in the ear-canal pressure produced by a pure tone[7].---	13
Figure.2(A)(B). The graphs to show the impulse response of the probe and suppressor for $f_s > f_p$ and $f_s < f_p$ conditions. -----	16
Figure.3. The graph of the time difference with respect to the ratio f_s/f_p with different swept rate r . -----	18
Figure.4(A). The picture of an Etymotic ER 10C probe. -----	21
Figure.4(B)(C). The picture of specially written python program for measurement. ---	22
Figure.4(D)(E)(F). The picture of specially written python program for measurement. -	23
Figure.4(G). The picture of an RME Fireface UCX sound card. -----	24
Figure.4(H). The picture of Python snippet for processing NF. -----	25
FIG.5. The virtual impulse responses of SFOAEs for different intensities in normally hearing subject s039(left ear). -----	26
Figure.6. Amplitude and phase of SFOAEs for different stimulus intensities in normally hearing subject s039(left ear). -----	27
Figure.7. The virtual impulse responses of SFOAEs for different intensities in normally hearing subject s040(left ear). -----	27
Figure.8. Amplitude and phase of SFOAEs for different stimulus intensities in normally hearing subject s040(left ear). -----	28
Figure.9. The virtual impulse responses of SFOAEs for different intensities in normally hearing subject s055(right ear). -----	28
Figure.10. Amplitude and phase of SFOAEs for different stimulus intensities in normally hearing subject s055(right ear). -----	29
Figure.11. The virtual impulse responses of SFOAEs for different intensities in normally hearing subject s055(left ear). -----	29
Figure.12. Amplitude and phase of SFOAEs for different stimulus intensities in normally hearing subject s055(left ear). -----	30
Figure.13. The “virtual” impulse responses with different sweep rates in normally hearing subject s039(left ear). -----	32
Figure.14. Amplitude and phase of SFOAEs for different sweep rates in normally hearing subject s039(left ear). -----	33
Figure.15. The “virtual” impulse responses with different sweep rates in normally hearing subject s040(left ear). -----	33
Figure.16. Amplitude and phase of SFOAEs for different sweep rates in normally hearing subject s040(left ear). -----	34

List of tables

Table1. Clarification of the nomenclature utilized of our experiments. -----	19
Table2. Measurement for SFOAE level effect. -----	20
Table3. Measurement for SFOAE rate effect. -----	21

List of abbreviations

OAEs	Otoacoustic emissions
SFOAEs	Stimulus-frequency otoacoustic emissions
DPOAEs	Distortion-product otoacoustic emissions
TEOAEs	Transient evoked otoacoustic emissions
SFE	Stimulus-frequency emission
SSS	Synchronized swept sines
NF	Noise floor
SPL	Sound pressure level

1. Introduction

Otoacoustic Emissions (OAEs) are sound signals generated by the ear, and Stimulus-frequency Otoacoustic Emissions (SFOAEs) are the type of OAEs which is generated if we stimulate the ear with a single tone. SFOAEs are a fundamental physiological phenomenon, providing valuable insights into the functioning of the auditory system [1]. They have traditionally been measured through established techniques such as nonlinear compression, two-tone suppression, and spectral smoothing.

The present study embarks on a critical exploration, seeking to ascertain the viability of a less conventional method: synchronized swept sines [8]. Unlike the well-documented approaches, swept sines offer the distinct advantage of ease of implementation and computational efficiency. This paper explores the application of synchronized swept sine technique as a novel approach for the extraction of SFOAEs. Swept sines are stimuli with continuously changing frequency. Our approach diverges by convolving the response with an inverse filter to produce a 'virtual' impulse response, enabling the identification of SFOAEs and their transformation into the frequency domain. While this technique has been successfully implemented in combination with compression method, as demonstrated in [2], its integration with the suppression method presents unique challenges. Specifically, the simultaneous presentation of a suppressor with the probe tone could potentially distort the response due to the proximity of impulse responses in the virtual domain. The temporal distance between the individual impulse responses decreases with increasing sweep rate and for suppressor to probe tone ratio approaching one. For example, in this thesis we used the ratio of 0.95. Therefore, this thesis aims to rigorously evaluate whether the synchronized swept sine technique, in conjunction with the suppression method, can effectively and accurately extract SFOAEs.

As mentioned, the distance between the impulse responses is influenced not only by the frequency difference between the suppressor and the probe tone but also by the rate of the swept sine. In addition, the SSS technique allows for testing the sweep rate effect on SFOAEs because it can be used also for high sweep rates (>2 oct/sec). Therefore, our study also delves into examining the effects of varying swept sine rates on the extraction and integrity of SFOAEs.

1.1 Organization of the thesis

In this thesis, Section 2 delves into the phenomena of SFOAEs, exploring the concepts of compression, suppression, and spectral smoothing. In Section 3, we discuss the application of Synchronized Swept Sine (SSS) technique in extracting SFOAEs, highlighting its methodological significance. Section 4, 'Methods', details our

experimental approach and presents our findings, particularly the impact of different stimulus intensities and sweep rates on SFOAEs as revealed by SSS. The thesis concludes with Section 5, summarizing our key findings and the problems we met in the results.

2. Stimulus frequency otoacoustic emissions

Otoacoustic emissions are acoustical signals generated from within the inner ear (cochlea). Stimulus frequency otoacoustic emissions (SFOAEs) are one of the types of otoacoustic emissions (OAEs) that are used in audiological and otological research.

The amplitude of SFOAEs is intrinsically linked to the level of cochlear amplification within the inner ear, with greater amplification correlating to higher SFOAE amplitudes. Additionally, SFOAEs have been posited as an objective methodology for assessing frequency selectivity of the inner ear, offering a non-invasive measure for evaluating cochlear function, as suggested in [3]. SFOAEs can provide information about the health and function of the outer hair cells in the cochlea, which are crucial for hearing. Damage or loss of these hair cells can result in hearing impairment.

SFOAEs occur in direct response to a specific tone or frequency presented to the ear. They are sounds that come out of the ear at the same frequency as the stimulus tone. SFOAEs are typically measured using a probe containing both a speaker and a microphone. A single frequency tone is presented to the ear via the speaker, and the microphone measures the sound that is reflected from the cochlea at the same frequency. If a suppressor is used to measure SFOAEs, it is presented simultaneously with the probe tone via the second speaker in the OAE probe to avoid nonlinear distortion generated due to nonlinear response of the probe speaker.

Differences from other OAEs: Shera and Guinan [10] proposed that OAEs arise by two fundamental mechanisms: nonlinear distortion and linear reflection. It is assumed that the main generation mechanism for SFOAEs is linear reflection. Nonlinear distortion is the generation mechanism for OAEs generated by two simultaneously presented tones; for distortion product otoacoustic emissions (DPOAEs) [4][10]. Linear reflection is assumed to be the main mechanism for another type of commonly used OAEs called transient evoked OAEs (TEOAEs), which are generated with a brief click or tone stimulus. SFOAEs have been suggested for using in combination with DPOAEs to provide a joint reflection distortion profile and classify the type of hearing loss [5].

2.1 Compression, suppression and spectral smoothing

SFOAEs have been meticulously measured employing a diverse range of techniques. Notably, these techniques include nonlinear compression, two-tone suppression, and spectral smoothing [7]. Each method offers a unique approach, capitalizing on distinct cochlear phenomena or specialized signal-processing techniques to elucidate the emission. However, all the three methods generally yield the same results as shown in [7]. The reason why we need to employ these methods is that the SFOAE is at the same frequency as the probe tone, so we must extract it (remove it from the response where we have also the response to the probe tone which evoked the emission).

Delving deeper into the methodologies, the nonlinear compression approach capitalizes on the difference in emission amplitude growth. Specifically, it observes the compressive increase of emission amplitude with the linear ascension of the stimulus. In this method, the emission is characterized as the intricate distinction between the ear-canal pressure observed at a singular intensity versus the rescaled pressure observed at an escalated intensity. At this escalated intensity, the emission is hypothesized to be minimal. As we can see in FIG.1, showing the amplitude of acoustical pressure measured in the ear canal, the quasiperiodic amplitude fluctuations are much smaller at high intensities than at low intensities. These fluctuations result from the interaction between the evoking probe tone and SFOAEs, which means that the SFOAE signal is weaker relative to the probe tone. In other words, FIG. 1 shows that SFOAE grows compressively with amplitude.

The suppression technique in SFOAE extraction involves the use of an additional tone, termed the 'suppressor,' which is specifically employed to diminish the BM response to the probe tone. When the BM response to the probe tone is effectively suppressed, the resultant SFOAE originating from the BM is absent, yet the evoking stimulus at the probe tone frequency persists. This allows for the isolation of SFOAE by subtracting the combined response to the probe tone and suppressor from the response to the probe tone alone. Typically, the suppressor's intensity exceeds that of the probe tone by at least about 15 dB, and at lower intensities, this difference can increase, for instance, to approximately 30 dB. The frequency of the suppressor is commonly set close to that of the probe tone, often with a ratio of f_s/f_p around 0.95. This methodology, as detailed in [6], provides a refined approach for the extraction of SFOAEs.

The third method, spectral smoothing, hinges on the convolution of the complex ear-canal pressure spectrum integrated with a designated smoothing function [7]. This method is particularly insightful as it leverages the latency disparities inherent between stimulus and emission. It mirrors the process of windowing in the associated latency domain.

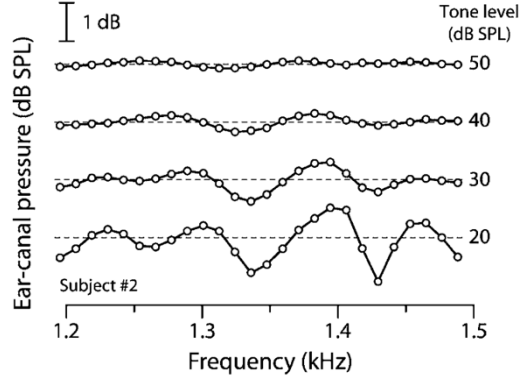


FIG. 1. The magnitude of the ear-canal pressure vs tone frequency at four different intensities is shown. Sound produced by the ear creates an intensity-dependent oscillatory fine structure that appears superposed on the constant stimulus background indicated by the dashed lines. Taken from [7].

Mathematically, the total ear-canal pressure, denoted as $P_{tot}(f; P_0)$, can be derived as the sum of its two constitutive elements: a stimulus-independent background and a frequency-modulated component, referred to as the "stimulus-frequency emission" (SFE). The relationship is given by:

$$P_{tot}(f; P_0) = P_0 + SFE(f; P_0). \quad (1)$$

a. Nonlinear Compression: Rooted in the principles of the compressive growth of SFOAE amplitude against the linear growth of the stimulus, the nonlinear compression approach capitalizes on the disparities at heightened stimulus levels (see FIG. 1). For precise estimation, the stimulus pressure, P_0^{com} , at high levels is scaled down linearly, yielding an accurate depiction of the SFOAE. This is summarized as:

$$SFE^{com} = P_{tot} - P_0^{com}. \quad (2)$$

b. Two-tone Suppression: This method measures SFOAE by nullifying the emission's contribution through a suppressor tone at a proximal frequency. The suppressor is believed to significantly diminish or eradicate the emission. Thus, the stimulus pressure, P_0^{sup} , is derived by subtracting the pressure from the suppressor tone. The formal representation is:

$$SFE^{sup} = P_{tot} - P_0^{sup}. \quad (3)$$

c. Spectral Smoothing: This technique harnesses advanced signal-processing methodologies. The primary aim is to alleviate spectral fluctuations resulting from interference between the stimulus and emission. Smoothing removes the fluctuations

visible in FIG. 1. The SFOAE is obtained by subtracting the smoothed pressure from the total pressure. Namely,

$$SFE^{sm} = P_{tot} - P_0^{sm}. \quad (4)$$

The study and measurement of SFOAEs, though intricate, is pivotal in advancing our understanding of auditory mechanisms. The triad of methodologies, while diverse in their techniques, offers a comprehensive view into the intricacies of SFOAEs, solidifying their significance in auditory science.

3. Synchronized swept sine for SFOAE measurement

The methodologies employed for the measurement of SFOAEs including suppression, compression, and spectral smoothing techniques. SSS technique is the technique for extraction of SFOAEs from swept sine response and should be used in combination with one of the mentioned methods. Swept sines can yield OAEs with high frequency resolution and many times lower recording time in comparison with steady-state tones [11]. After the response to swept stimulus is recorded, various techniques exist for stimulus extraction, e.g. least-square fitting technique [11], heterodyne-technique [12].

The synchronized swept-sines (SSS) technique, as pioneered by Novak et al [8], is an innovative method tailored for the analysis of nonlinear systems. These SSSs represent a specific subset of exponential or as often referred to, logarithmic swept-sine signals[8]. The versatility of the SSS methodology allows for its application in deciphering nonlinear systems, particularly in the context of block-oriented models like the Generalized Hammerstein models or Diagonal Volterra Series.

A notable attribute of the SSS technique is its capacity to distinctly segregate frequency-dependent higher harmonics. This inherent quality offers the added advantage of mitigating complexities tied to overlapping frequency components. Moreover, the practicality of the SSS technique is underscored by its computational efficiency and its adaptability regardless of the nature of the nonlinearity in the system under study.

Its unique capability to distinguish between OAE components with varied latencies [9] further augments the potential of the SSS technique, positioning it as a potent tool for SFOAE measurements. This thesis tries to delve deeper into the efficacy of the SSS methodology.

Synchronized Swept-Sine (SSS)

The Synchronized Swept-Sine (SSS) [9] signal can be conceptualized as a distinctive variant of the exponential swept-sine, mathematically described as:

$$s(t) = \sin(\varphi(t)). \quad (5)$$

Where the phase, $\varphi(t)$, is given by:

$$\varphi(t) = 2\pi f_a L \exp\left(\frac{t}{L}\right). \quad (6)$$

A salient feature of this signal is its coefficient L , which serves as an indicator of the sweep rate, defined as:

$$L = \frac{T}{\ln\left(\frac{f_b}{f_a}\right)}. \quad (7)$$

In this equation, f_a and f_b symbolize the initial and terminal frequencies, respectively, with corresponding timestamps $t = 0$ and $t = T$.

One of the distinguishing attributes of this swept-sine is its intrinsic relationship with higher-order harmonics, specifically, frequencies that are whole-number multipliers of the base frequency. As delineated in [8], when the phase $\varphi(t)$ is multiplied by an integer m , the result corresponds to the generation of the m position harmonic of the swept sine. This action is analogous to introducing a phase lag of Δt_m , expressed as:

$$m\varphi(t) = \varphi(t - \Delta t_m). \quad (8)$$

With the relationship:

$$\Delta t_m = -L \ln(m). \quad (9)$$

Subsequently, a higher-order harmonic version of the SSS can be articulated as:

$$s_m(t) = \sin(m\varphi(t)) = \sin(\varphi(t - \Delta t_m)). \quad (10)$$

The utility of the SSS lies predominantly in its proficiency for discerning frequency-contingent higher harmonics (as emphasized in [8]) and its potential in estimating frequency-conditional intermodulation effects [9].

Following the measurement process and the acquisition of the output signal $y(t)$, we retrieve the impulse response $h(t)$ through the application of a deconvolution technique. The convolution in the frequency domain as $Y(f) = S_1(f)H(f)$, where $S_1(f)$ is the Fourier transform of the SSS $\sin(\varphi_1(t))$. We got the analytical form of it, which we derived from [8], namely:

$$S_1(f) = \frac{1}{2} \sqrt{\frac{L}{f}} \exp\left\{j2\pi f L \left[1 - \ln\left(\frac{f}{f_p}\right)\right] - j\frac{\pi}{4}\right\}, \quad (11)$$

where f_p is the starting frequency of the probe tone. The impulse response $h(t)$ is then obtained using frequency domain deconvolution as:

$$h(t) = \mathcal{F}^{-1}\left\{\frac{Y(f)}{S_1(f)}\right\}. \quad (12)$$

This will yield the virtual impulse response which contains SFOAE at $t = 0$.

If the tone is swept upward in frequency and $f_s > f_p$, the response to the stimulus f_s

occurs temporally prior to the response to the stimulus f_p within the impulse response. Our preliminary data suggests that the response to the suppressor can be rendered virtually imperceptible through this technique. I have made a graph to show the impulse response of the probe and suppressor for this condition.

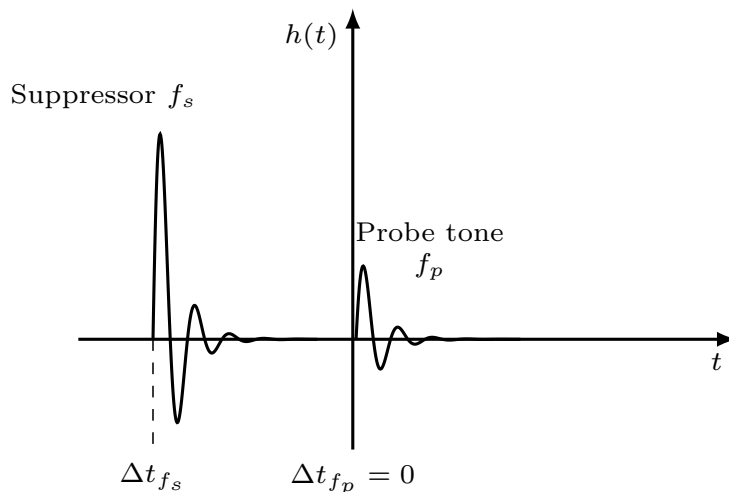


FIG.2(A). The graph to show the impulse response of the probe and suppressor for $f_s > f_p$ condition.

Conversely, if $f_s < f_p$, the response to f_s occurs after the response to f_p , with the ideal temporal separation being at least 30 milliseconds post the f_p response.

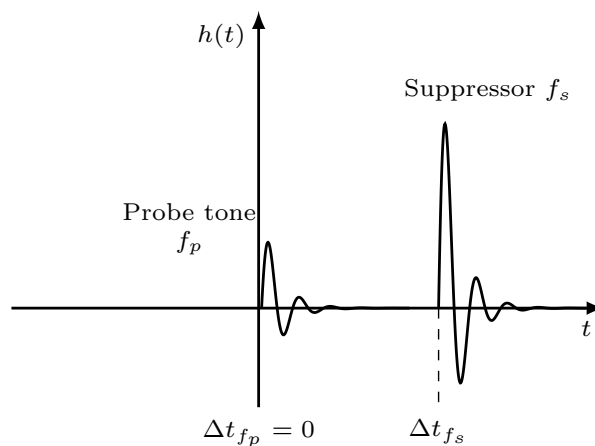


FIG.2(B). The graph to show the impulse response of the probe and suppressor for $f_s < f_p$ condition.

In the measurement of SFOAEs using a suppressor, the phase of the suppressor is altered across repeated trials to facilitate its removal from the final response. This technique, referred to as the modified, interleaved suppression paradigm, is outlined in [10]. When paired with the SSS technique, it's expected to produce a refined impulse response highlighting the SFOAE component exclusively. However, fluctuations in ear impedance, possibly from the middle ear muscle reflex, may result in remnants of both the suppressor and the probe tone within the captured response. This thesis evaluates the effectiveness

of the SSS method in extracting SFOAEs when employing this modified, interleaved suppression paradigm.

It is important to note that when conducting a frequency sweep from high to low, the temporal relationship between the responses to f_s and f_p is inverted. In this case, if $f_s > f_p$, the response to f_s follows the response to f_p , whereas if $f_s < f_p$, the response to f_s precedes the response to f_p . Recognizing the advantages of having the response to f_p consistently follow the response to f_s , we therefore recommend employing a downward frequency sweep when the objective is to have $f_s < f_p$. So, we decided to focus in this thesis only on this suppressor-probe tone combination and downward sweeping condition.

We sweep a sine exponentially between f_s and f_p frequencies, the sweep rate r described in octaves per second determines the temporal difference between probe impulse response and suppressor impulse response of the swept sine, namely,

$$\Delta t = L \cdot \ln\left(\frac{f_s}{f_p}\right). \quad (13)$$

and

$$L = \frac{1}{r \cdot \ln(2)}. \quad (14)$$

From (13) and (14), we can see that only the ratio (f_s/f_p) and sweep rate (r) determines the temporal difference between the probe tone and suppressor tone impulse responses in the virtual impulse response. So as a first step, we make a graph (see Fig. 3(b)) showing the dependence of Δt on $\frac{f_s}{f_p}$ for different sweep rates $r = 1, 2, 4, 8$. Displaying values of

$\frac{f_s}{f_p}$ exceeding 2 is not necessary, because such a large ratio is infrequently employed in SFOAE measurements because it yields SFOAEs which probably do not originate from the best frequency place of the probe tone traveling wave. It would be better to emphasize the region corresponding to approximately 30ms latency within the graph, given the fact that latencies in human SFOAEs are commonly within this range [7].

However, additional scenarios may arise contingent upon the directionality of the frequency sweep, whether it proceeds from low to high frequencies or conversely, from high to low frequencies. So therefore, FIG.3 shows the 30 ms limit with a dashed line in both half-planes: for $\Delta t < 0$ and for $\Delta t > 0$. From FIG.3, we can see that for frequency ratio 0.95, the "safe" sweep rate yielding a sufficient distance between suppressor impulse response and probe tone impulse response is up to the sweep rate of 2 [oct/sec].

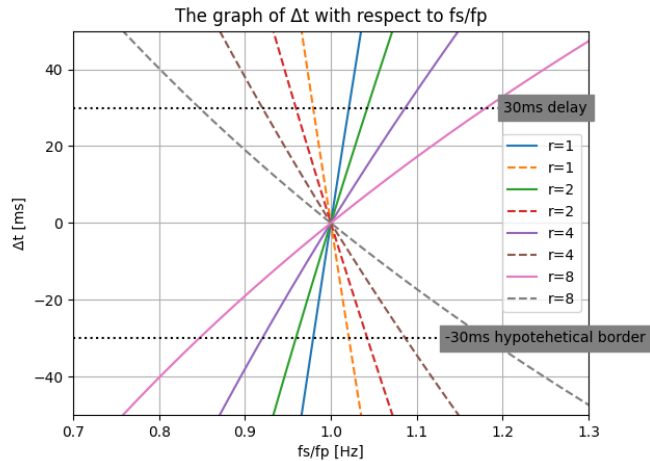


FIG.3. The graph of the time difference between f_s and f_p impulse responses with respect to the ratio $\frac{f_s}{f_p}$ for different swept rates r .

From the graph, we can see that for frequency ratio 0.95, the “safe” sweep rate yielding a sufficient distance between suppressor impulse response and probe tone impulse response is up to the sweep rate of 2 [oct/sec].

4. Methods

In this section, we introduce the experimental methodology. We measured the effect of stimulus intensity and the effect of swept sine rate on SFOAEs derived from swept sine response by using the SSS technique.

4.1. Subject

We place a particular emphasis on the selection of our experimental subjects, as the validity and reliability of our data are inextricably tied to their auditory health.

We conducted a measurement of the left ear of our subject, identified by the pseudonym 's039'. His pure tone hearing thresholds were within the range of 15 dB re hearing level for frequencies between 0.25 and 8 kHz. The age of the subject is 24. Then we conducted a measurement of the left ear on myself, identified by the pseudonym 's040'. My pure tone hearing thresholds were within the range of 15 dB re hearing level for frequencies between 0.25 and 8kHz. The age of this subject is 23. We also conducted a measurement

on the subject 's055' for both the left ear and the right ear. His pure tone hearing thresholds were within the range of 15 dB re hearing level for frequencies between 0.25 and 8kHz.

4.2. Stimuli

Prior to delineating the specifics of the experimental protocol, it is essential to clarify the nomenclature utilized within the scope of our study. Note that Table1 describes the variable names and their meanings used in the attached python codes below.

fpb	Denotes the probe's start frequency, establishing the initial point of our frequency range for the probe tone.
fpe	Refers to the probe's end frequency, marking the terminal frequency in our probe tone spectrum.
fsfp	The ratio between the suppressor and probe tone frequencies, a crucial factor in defining the relationship and interaction between these two auditory stimuli.
fsb	Calculated as fpb multiplied by fsfp, represents the suppressor's start frequency, indicating the commencement frequency for the suppressor tone.
fse	Derived as fpe multiplied by fsfp, signifies the suppressor's stop frequency, and demarcates the cessation point for the suppressor tone within the experimental frequency range.
Lp	The intensity of the f1 tone, measured in decibels, serving as a quantifiable measure of the probe tone's loudness.
Ls	Indicates the intensity of the f2 tone, also in decibels, which quantifies the loudness of the suppressor tone.
r	The sweep rate, expressed in octaves per second, which defines the speed at which the frequency sweep occurs throughout the experiment.

Table1. Clarification of the nomenclature utilized within the scope of our experiments.

Each of these parameters plays a pivotal role in the configuration of our auditory assessment, thereby allowing for a controlled and precise examination of the subject's otoacoustic emissions, with particular attention to the SFOAEs.

We could also calculate the duration of the stimuli which depends on the swept sine rate, by using the equation:

$$T = \frac{\log_2\left(\frac{f_2}{f_1}\right)}{r}. \quad (15)$$

For example, in Table1 below, the swept sine rate $r = 1$. So, the duration of the stimuli in this case is $T = \frac{\log_2\left(\frac{4000}{500}\right)}{1} = 3s$.

First, we measured for SFOAE level effect. We measured the data from the left ear of s039, s040 and both the left and right ear of s055.

f _{pb} = 4000Hz, f _{pe} = 500Hz (Downward sweep)		
fsfp = 0.95		
r = 1 octave per second		
$T = 3s$		
Measurement for SFOAE level effect in the left ear of s039, s040.	Lp [dB SPL]	Ls [dB SPL]
	20	50
	30	50
	40	55
Measurement for SFOAE level effect in the left ear of s055.	50	65
	20	50
	30	50
	40	55
Measurement for SFOAE level effect in the right ear of s055.	45	60
	20	50
	30	50
	40	55
	50	65

Table2. Measurement for SFOAE level effect.

Second, we measured for SFOAE sweep rate effect. We again measured the data from the left ear of s039 and s040.

f _{pb} = 4000Hz, f _{pe} = 500Hz (Downward sweep)				
f _{sfp} = 0.95				
Measurement subject	L _p [dB SPL]	L _s [dB SPL]	r [octaves per second]	T [s]
Measurement for SFOAE rate effect on s039.	30	50	1	3
	30	50	2	1.5
	30	50	4	0.75
	30	50	8	0.375
Measurement for SFOAE rate effect on s040.	45	60	1	3
	45	60	2	1.5
	45	60	4	0.75
	45	60	8	0.375

Table3. Measurement for SFOAE rate effect.

4.3. Data acquisition

The specialized equipment includes:

1. An Etymotic ER 10C probe, which is renowned for its precision in capturing otoacoustic emissions within a controlled environment, thus ensuring the fidelity of the auditory data captured.



FIG.4(A). The picture of an Etymotic ER 10C probe. Picture taken from [13].

2. A bespoke Python software suite, meticulously developed for the purpose of this measurement, which facilitates the nuanced control and data acquisition necessary for such sensitive auditory examinations.

```

1 import numpy as np
2 import matplotlib.pyplot as plt
3 import os
4 from scipy.io import savemat
5 from UserModules.pySFOAEmodule import sendChirpToEar
6
7 fsamp = 44100
8 MicGain = 40
9 xxx, Hinear1, Hinear2, fxinear, y1, y2 = sendChirpToEar(AmpChirp=0.05,fsamp=fsamp,MicGain=MicGain,Nchirps=300,bufferSize=2048,latency_SC=8236)
10 #AmpChirp=0.01,fsamp=44100,MicGain=40,Nchirps=300,bufferSize=2048,latency_SC=8236
11
12
13 pathfolder = 'Calibration_files/Files'
14 if not os.path.exists(pathfolder):
15     os.makedirs(pathfolder)
16 filename = 'InEarCalData'
17 caldata = {'Hinear1':Hinear1,'Hinear2':Hinear2,'fxinear':fxinear}
18 savemat(pathfolder + '/' + filename + '.mat', caldata)
19
20
21 fig,ax = plt.subplots()
22 ax.semilogx(fxinear,np.abs(Hinear1))
23 ax.semilogx(fxinear,np.abs(Hinear2))
24
25
26
27 fig,ax = plt.subplots()
28 ax.plot(y1)
29 ax.plot(y2)
30
31 plt.show()

```

```

1 import numpy as np
2 from scipy.io import savemat
3 import keyboard
4 import tty
5 import termios
6 import sys
7 import datetime
8 from UserModules.pySFOAEmodule import RMEplayrec, generateSSSPHase, calcDPgram
9 from UserModules.pyUtilities import butter_highpass_filter
10 #from matplotlib.pyplot import Figure
11 import matplotlib.pyplot as plt
12 # parameters of evoking stimuli
13
14 fpb = 4000 # fprobe start frequency
15 fpe = 500 # fprobe end frequency
16 fsfp = 0.95 # ratio between suppressor and probe tone frequency
17 fsb = fpb*fsfp # fsuppressor start frequency
18 fse = fpe*fsfp # fsuppressor stop frequency
19 phasep = 0
20 phases = 0
21 Lp = 45 # intensity of f1 tone
22 Ls = 60 # intensity of f2 tone
23 r = 8 # sweep rate in octaves per second
24 fsamp = 44100 # sampling frequency
25 fsamp = 96000; bufsize = 4096; latency_SC = 16448 # sampling frequency
26 micGain = 40

```

```

27 ear_t = 'L' # which ear
28 save_path = 'Results/sxxx/'
29 #save_path = 'Results/pokus/'
30 subj_name = 'sxxx'
31
32 def get_time() -> str:
33     # to get current time
34     now_time = datetime.datetime.now().strftime('%Y_%m_%d_%H_%M_%S')
35     return now_time
36
37
38 # data initialization
39
40 # generate stimuli
41 #s1,s2 = generateDPOAEstimulus(f2f1, fsamp, f2b, f2e, r, L1, L2)
42 ProbeSpeakerP = 1
43 ProbeSpeakerS = 2
44 sp = generateSSSPHase(fsamp, fpb, fpe, phasep, r, Lp, ProbeSpeakerP)
45 ss = generateSSSPHase(fsamp, fsb, fse, phases, r, Ls, ProbeSpeakerS)
46
47 fig,ax = plt.subplots()
48 ax.plot(sp[:10000])
49 fig,ax = plt.subplots()
50 ax.plot(ss[:10000])
51 sp_in = np.vstack([sp,0*sp,sp]).T # make 3 chan input for probe
52 sps_inP = np.vstack([sp,ss,sp+ss]).T # make 3 chan input for
53 sps_inN = np.vstack([sp,-1*ss,sp+ss]).T # make matrix where the first column

```

```

54 if fpb<fpe:
55     numfoct = np.log2(fpe/fpb) # number of octaves for upward sweep
56 else:
57     numfoct = np.log2(fpb/fpe) # number of octaves for downward sweep
58
59
60 T = numfoct/r # time duration of the sweep for the given sweep rate
61
62 t = get_time() # current date and time
63
64 # measurement phase
65 counter = 0
66 |
67 try:
68     while True:
69         recsig_sp1 = RMEplayrec(sp_in,fsamp,SC=21,buffersize=bufsize) # send signal to the sound card
70
71         recsig_spsP = RMEplayrec(sps_inP,fsamp,SC=21,buffersize=bufsize) # send signal to the sound card
72
73         recsig_sp2 = RMEplayrec(sp_in,fsamp,SC=21,buffersize=bufsize) # send signal to the sound card
74
75         recsig_spsN = RMEplayrec(sps_inN,fsamp,SC=21,buffersize=bufsize) # send signal to the sound card
76         counter += 1
77         print('Rep: {}'.format(counter))
78         # every recorded response is saved, so first make a dictionary with needed data
79         data = {"recsig_sp1": recsig_sp1,"recsig_sp2": recsig_sp2,"recsig_spsP": recsig_spsP,"recsig_spsN": recsig_spsN,"fsamp":fsamp,\
80               "fsfp":fsfp,"fpb":fpb,"fpe":fpe,"r":r,"Lp":Lp,"Ls":Ls} # dictionary

```

```

81     if counter<10: # to add 0 before the counter number
82         counterSTR = '0' + str(counter)
83     else:
84         counterSTR = str(counter)
85
86     file_name = 'swSFOAE_' + subj_name + '_' + t[2:] + '_' + 'Fpb' + '_' + str(fpb) + 'Fpe' + '_' + str(fpe) + 'Lp' + '_' + str(Lp) + 'dB' + '_' + \
87     'Ls' + '_' + str(Ls) + 'dB' + '_' + 'fsfp' + '_' + str(fsfp * 100) + '_' + '0ct' + '_' + str(r * 10) + '_' + ear_t + '_' + counterSTR
88     savemat(save_path + '/' + file_name + '.mat', data)
89
90 except KeyboardInterrupt:
91     print("KeyboardInterrupt received. Exiting the loop.")
92 except Exception as e:
93     print(f"An error occurred: {e}")

```

FIG.4(B)(C)(D)(E)(F). The picture of specially written python program for measurement.

3. An RME Fireface UCX sound card, selected for its exemplary audio fidelity, which serves as the cornerstone of our auditory signal processing. And for communication with sound card, we used a Python module called sound device (connected) [14].



FIG.4(G). The picture of an RME Fireface UCX sound card.

The primary factor that could potentially perturb our measurement is the ringing in the impulse response resulting from the suppressor. However, this can be significantly mitigated by employing the modified, interleaved suppression paradigm [10], given by:

$$p_{SFOAE} = \frac{(p_1 + p_2 - (p_{s1} + p_{s2}))}{2}$$

In this equation, p_1 and p_2 is ear canal pressure with probe tone only (without suppressor), whereas p_{s1} is ear canal pressure with probe tone and suppressor (simultaneously) and p_{s2} is the ear canal pressure with probe tone and suppressor with altered phase (180 phase shifted in comparison to p_{s1}). The method aims to isolate the otoacoustic emission itself by canceling out the effect of the suppressor tone. This is achieved by taking the difference between the emissions measured with and without the suppressor and then averaging. The idea is that the suppressor effect will be present in both measurements but the otoacoustic emission will only be in the non-suppressed measurements. Subtracting these gives the pure otoacoustic emission response.

Subsequent experimental sessions were executed in November, involving myself (s040) and another subject (s055). The investigative procedures administered to subject 's040' replicated the methodology previously applied to subject 's039'. And the experimental paradigm for subject 's055' omitted the sweep rate analysis and incorporated an additional cohort of tests specifically targeting the auditory responses of the right ear.

4.4. NF (Noise floor) processing

```
dt = -fsamp*L1sw*np.log(1) # positions of the selected IMD component [samples]
dt_ = round(dt)
dt_rem = dt - dt_
hmfftlen = 2**12
len_IRpul = int((hmfftlen)/2) # length of the impulse response window (adequate for the used time windows for SFOAEs)
if dt_ >= 0: # downward sweep
    hm = np.concatenate((h[dt_-len_IRpul:],h[:dt_+len_IRpul]))
    hmNoise = h[2*(dt_+len_IRpul):dt_+4*len_IRpul]
else: # upward sweep
    hm = h[len(h)+dt_-len_IRpul:len(h)+dt_+len_IRpul]
    hmNoise = h[2*len(h)+dt_-len_IRpul:2*len(h)+dt_+len_IRpul]
```

FIG.4(H). The picture of Python snippet for processing NF.

This piece of code is part of our Python program for processing audio data, specifically for analyzing noise in the context of SFOAEs measured during auditory tests. The input to the function is for the noise case a noise matrix. We made a noise matrix by subtracting the median across individual responses and then from the mean value of the noise matrix we calculate virtual impulse response in the same way as for the SFOAE signal. But the difference is that we window the impulse response for slightly later times than in case of SFOAE signal, in the sample which is at 2×2^{12} sample after the starting sample for $t = 0$. The further the SFOAEs line is from the NF line, it means that the obtained SFOAEs are less affected by noise and are more observable.

5. Results

The synchronized swept sine technique adeptly transforms the recorded response induced by a swept sine stimulus into a "virtual" impulse response, as depicted in Figures 2(A) and 2(B). This transformation facilitates the distinct delineation of the impulse response attributable to the probe tone as well as that of the suppressor, contingent upon its presentation. The temporal separation between these responses, denoted as Δt , is linked to the rate of the swept sine and the frequency ratio between the suppressor and probe tone, as mentioned in the equation (13), (14) we introduced in the previous content. In the context of Stimulus Frequency Otoacoustic Emissions (SFOAEs), the frequency differential is customarily minimal (for instance, a ratio of $f_s/f_p = 0.95$ as employed in this paper). Consequently, this research tries to ensure the applicability of the synchronized swept sine technique to the measurement of SFOAEs when a suppressor is utilized.

5.1 Effect of stimulus intensity on SFOAEs extracted by SSS

For the measurement, we used modified, interleaved suppression paradigm [10] in which the suppressor is presented with altered phase to cancel it from the resulting response. If the canceling works correctly, we can use SSS technique for SFOAEs measured using suppressors without any “restriction” or limit on the swept sine sweep rate. However, any fluctuation in the input impedance of the ear can cause incomplete cancelation of the suppressor in the resulting “virtual” impulse response. Therefore, this section presents SFOAEs measured using the SSS technique and suppressor of various probe tone (L_p) and suppressor (L_s) intensities. Stimulus at larger intensities can active the middle ear reflex and alter the ear impedance.

SFOAEs in time domain and frequency domain for s039

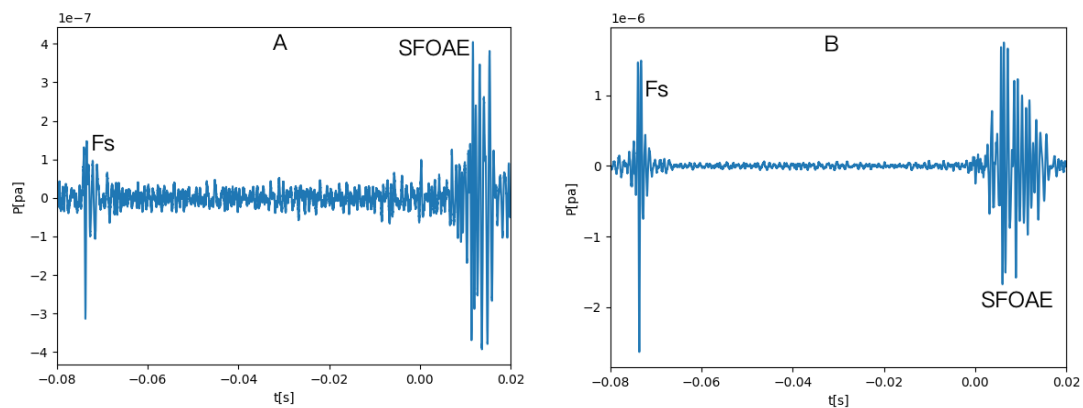


FIG.5. The virtual impulse responses of SFOAEs for different intensities in normally hearing subject s039(left ear). The stimulus parameters for A were $L_p=20$ dB SPL, $L_s=50$ dB SPL; for B were $L_p=50$ dB SPL, $L_s=65$ dB SPL.

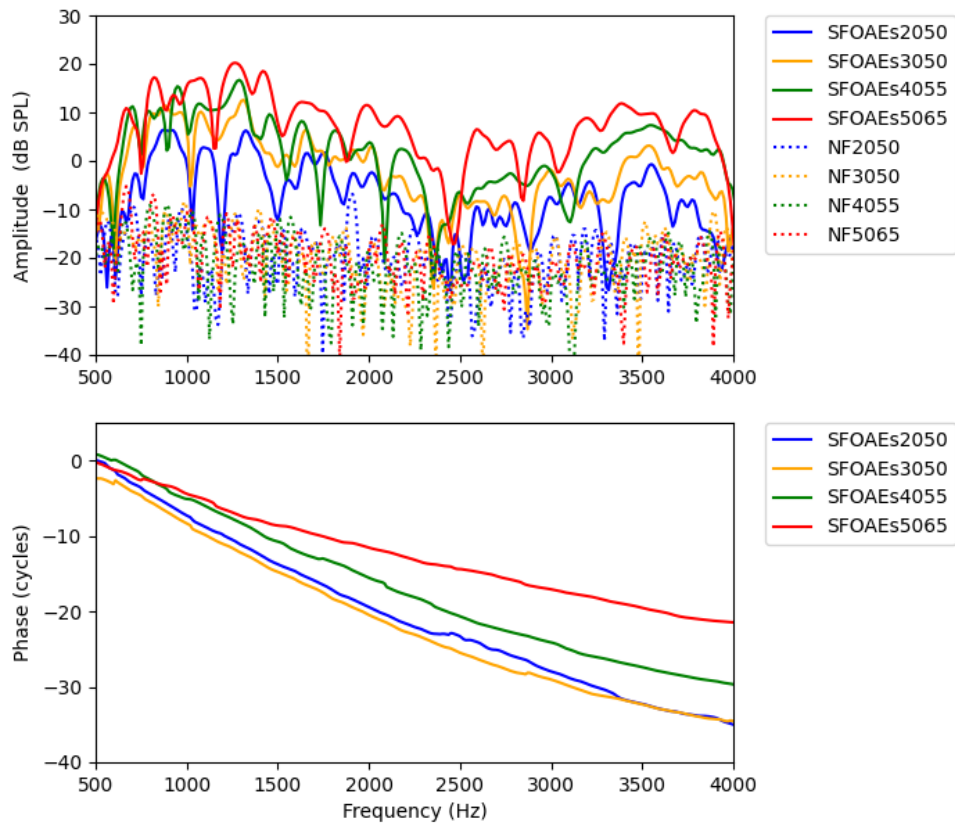


FIG.6. Amplitude and phase of SFOAEs for different stimulus intensities. SFOAEs were extracted from the ear canal responses evoked with SSS in normally hearing subject s039(left ear). The stimulus parameters are shown in the figure. In the legend, the first number depicts L_p and the second number depicts L_s . The solid lines with different colors and the dotted lines with different colors, respectively, depict SFOAEs and NF extracted by the SSS technique.

SFOAEs in time domain and frequency domain for s040

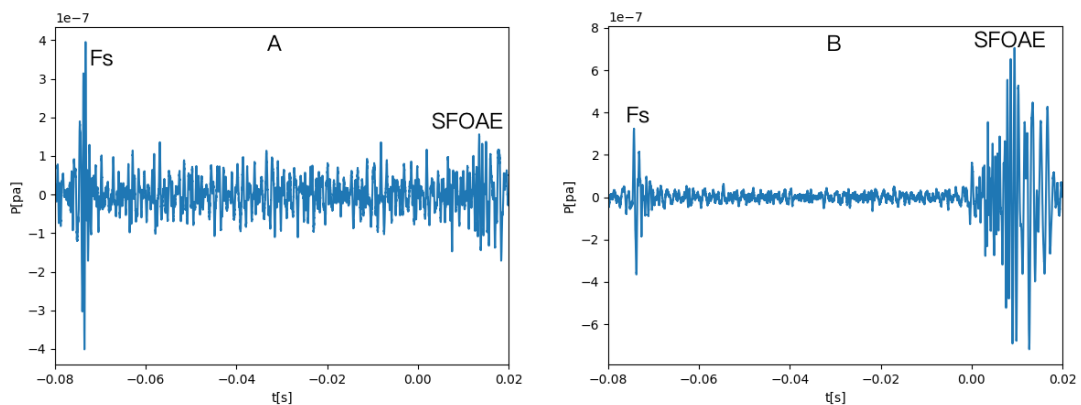


FIG.7. The virtual impulse responses of SFOAEs for different intensities in normally hearing subject s040(left ear). The stimulus parameters for A were $L_p=20$ dB SPL, $L_s=50$ dB SPL; for B were $L_p=50$ dB SPL, $L_s=65$ dB SPL.

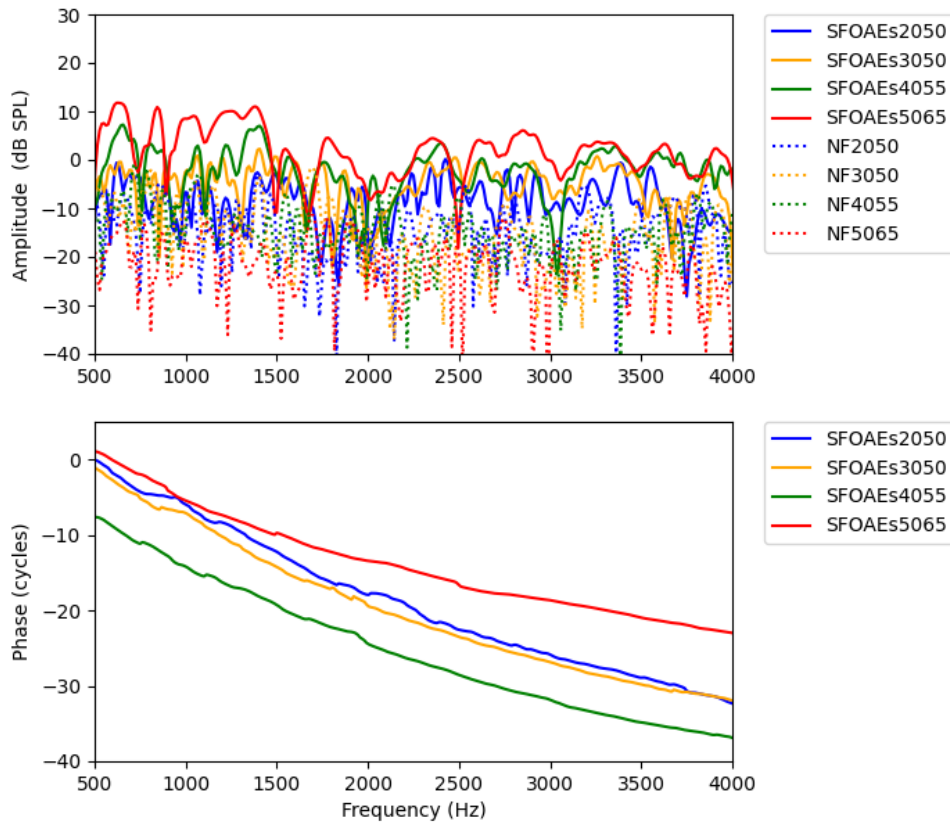


FIG.8. Amplitude and phase of SFOAEs for different stimulus intensities. SFOAEs were extracted from the ear canal responses evoked with SSS in normally hearing subject s040(left ear). The stimulus parameters are shown in the figure. In the legend, the first number depicts L_p and the second number depicts L_s . The solid lines with different colors and the dotted lines with different colors, respectively, depict SFOAEs and NF extracted by the SSS technique.

SFOAEs in time domain and frequency domain for s055

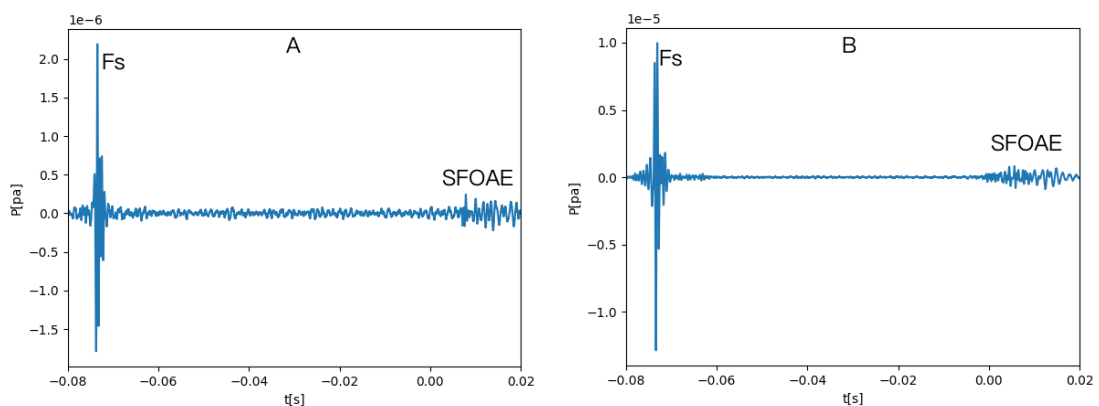


FIG.9. The virtual impulse responses of SFOAEs for different intensities in normally hearing subject s055(right ear). The stimulus parameters are shown in the figure. The stimulus parameters for A were $L_p=20$ dB SPL, $L_s=50$ dB SPL; for B were $L_p=50$ dB SPL, $L_s=65$ dB SPL.

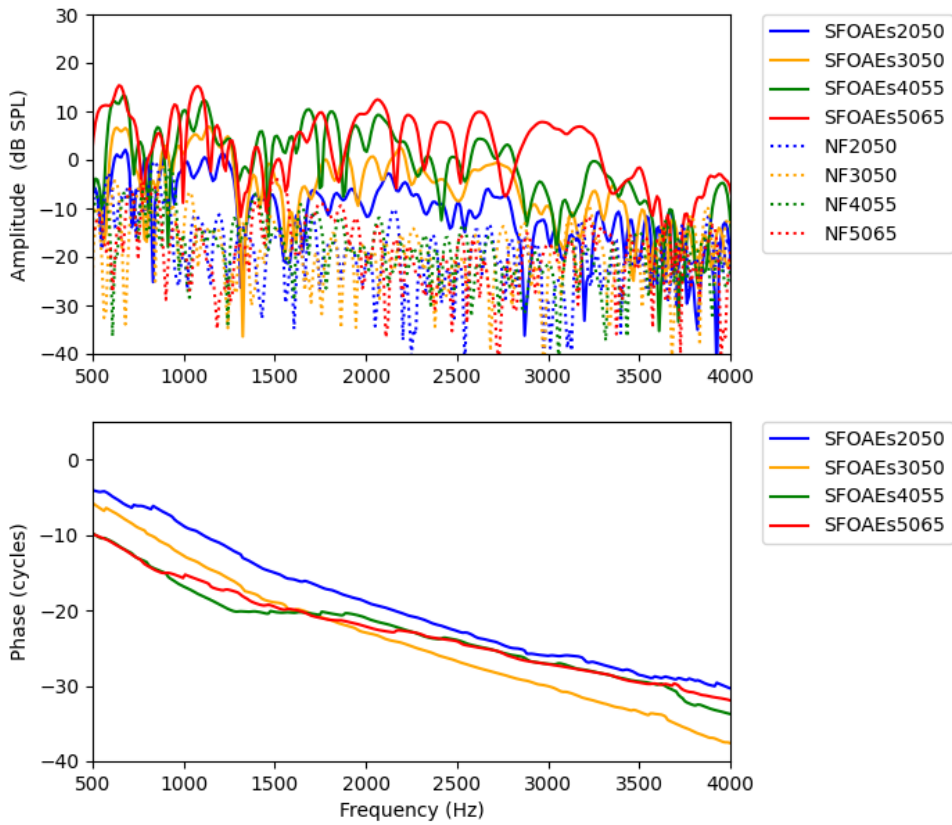


FIG.10. Amplitude and phase of SFOAEs for different stimulus intensities. SFOAEs were extracted from the ear canal responses evoked with SSS in normally hearing subject s055(right ear). The stimulus parameters are shown in the figure. In the legend, the first number depicts L_p and the second number depicts L_s . The solid lines with different colors and the dotted lines with different colors, respectively, depict SFOAEs and NF extracted by the SSS technique.

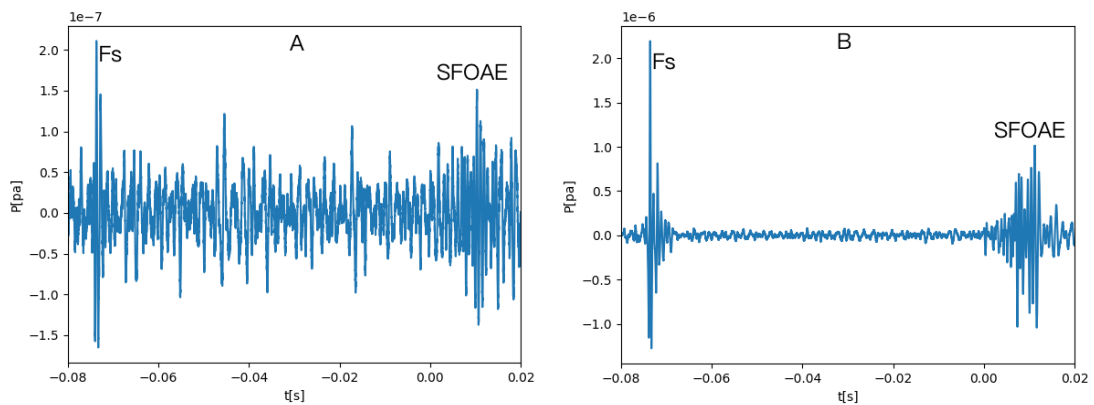


FIG.11. The virtual impulse responses of SFOAEs for different intensities in normally hearing subject s055(left ear). The stimulus parameters are shown in the figure. The stimulus parameters for A were $L_p=20$ dB SPL, $L_s=50$ dB SPL; for B were $L_p=50$ dB SPL, $L_s=65$ dB SPL.

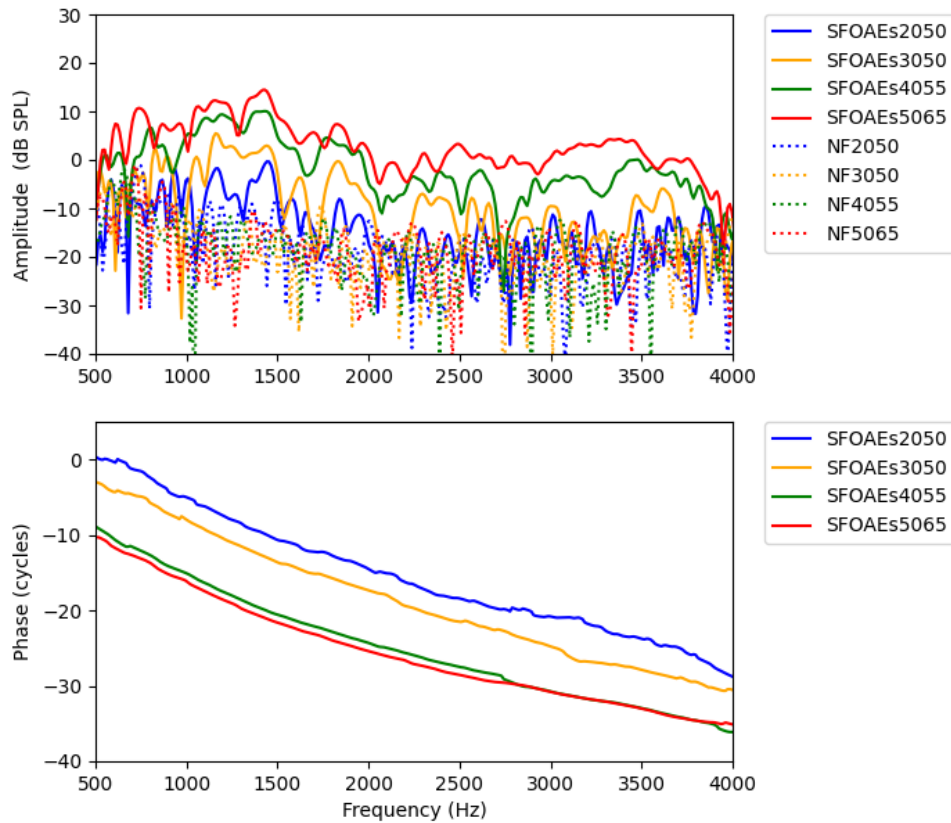


FIG.12. Amplitude and phase of SFOAEs for different stimulus intensities. SFOAEs were extracted from the ear canal responses evoked with SSS in normally hearing subject s055(left ear). The stimulus parameters are shown in the figure. In the legend, the first number depicts L_p and the second number depicts L_s . The solid lines with different colors and the dotted lines with different colors, respectively, depict SFOAEs and NF extracted by the SSS technique.

SFOAEs in the time domain:

The FIG.5, FIG.7, FIG.9, FIG11 are the virtual impulse responses of SFOAEs at different stimulus intensities in the time domain. In A panel of figures, L_p is set to 50 dB SPL, and in B panel of figures, it is increased to 65 dB SPL. The suppressor tone, which is located around $t = -73\text{ms}$ before zero time (F_s).

SFOAEs should be located somewhere between $t = 0$ and $t = 30\text{ms}$. In our figures, SFOAEs are located somewhere around $t = 10\text{ms}$. And the rest part of the figure (between F_s and SFOAEs) is the background noise. For all the subjects, we can see that as the probe level increases, the peak value of the SFOAE waveform increases significantly.

If the modified, interleaved suppression paradigm [10] is correct, then there should no suppressor response visible in these virtual impulse responses. But we can see it and it is much larger for $L_s = 65$ dB SPL than for $L_s = 50$ dB SPL. So, we suggest that this indicates that the middle ear muscle reflex could be activated for larger suppressor intensity, and this affects or hamper or the ability of the interleaved suppression paradigm [10] to cancel the suppressor response. However, we are showing that these remnants or residual suppressor responses are still relatively small, and we assume that they do not affect SFOAEs.

As we already said, the presence of suppressor or its remnants in the the 'virtual' impulse responses for larger stimulus intensities may indicate activation of the middle-ear muscle reflex. If this is true, another advantage of the SSS technique is that it indicates this activation. It can be employed during SFOAE analysis and mainly during interpretation of the results. Notice that at larger intensities, the time domain SFOAEs (B panel of FIG.5,7,9,11) contain significant amount of energy zero latencies (near $t = 0$), which may also be due to middle-ear muscle reflex activation.

SFOAEs in the frequency domain:

The FIG.6, FIG.8, FIG.10, FIG.11 are the amplitude and phase figure of SFOAEs for different probe intensity (L_p). The suppressor intensity L_s was 50 dB SPL for L_p smaller than 30 dB SPL and then above this level, the suppressor intensity was 15 dB SPL above the probe tone intensity. SFOAEs were extracted by the SSS technique from swept sine responses recorded in the ear of normally hearing subjects s039, s040, s055.

These graphs display data related to SFOAEs across a range of frequencies, presented in two parts: amplitude and phase. Both graphs are plotted with frequency on the x-axis, which spans from 500 Hz to 4000 Hz. The top graph illustrates the amplitude of the SFOAEs in dB SPL (Sound Pressure Level) across the frequency spectrum.

The amplitude across all conditions appears to be highest at lower frequencies and gradually decreases as the frequency increases. There is a noticeable variability or "ripple" in the amplitude across the frequency range, this amplitude fine structure is typically seen in SFOAEs. SFOAEs are caused by the mechanism of linear reflection from irregularities along the organ of Corti. These irregularities are randomly distributed and backscatter the wavelets with different phases. The resulting SFOAE amplitude is then therefore determined not only by the amplitude of these wavelets, but also by their phase, i.e. whether they add coherently or destructively.

We also know that larger the level difference between the SFOAE amplitude and noise floor, obtained SFOAEs are less affected by noise and are more observable. So, we can see that as the probe tone level increases, the SFOAE amplitude increases. This increase is approximately linear at the lowest intensities and then may saturate. We see this trend in our data, which suggests a reliable measurement or a common characteristic across different test subjects or repeated measurements. The bottom graph shows the phase of the SFOAEs in cycles. The phase slope determines the latency of the emission.

As mentioned above, SFOAEs are generated by the mechanism of reflection from irregularities. The phase slope can be used to calculate round trip travel time of the wave towards the place along the BM from which the wave is backscattered and the travel time of the backscattered wave into the stapes and then to the outer ear where the wave is recorded by the probe microphone. The latency correlates with sharpness of tuning in cochlear filters [3]. As the intensity increases, the phase slope is shallower, latency is smaller. This possibly reflects the growing bandwidth of cochlear filters as intensity

increases and shift of the traveling wave amplitude towards base as intensity increase.

Our figures revealed that at a low L_p (20 dB SPL), SFOAEs were a bit masked by noise. Conversely, at a higher L_p (50 dB SPL), SFOAEs were notably more distinguishable against the background noise. This distinction was proven again by frequency domain figures, where at a higher L_p , a greater separation between the solid lines representing SFOAEs and the dotted lines representing NF.

5.2 Effect of sweep rate on SFOAEs extracted by SSS

SFOAEs in time domain and frequency domain for s039

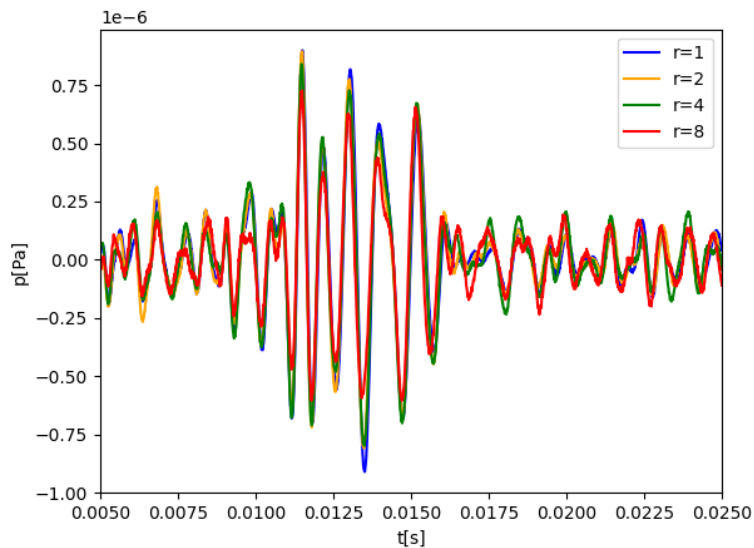


FIG.13. The "virtual" impulse responses showing SFOAEs in the time domain for different sweep rates for subject s039(left ear).

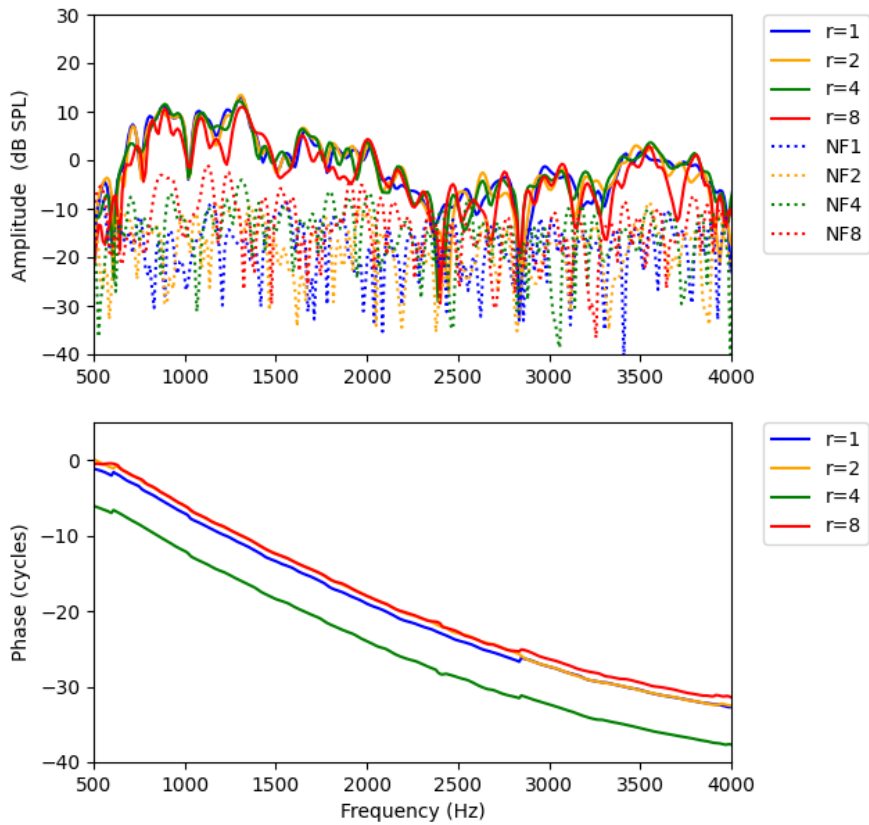


FIG.14. Amplitude and phase of SFOAEs for different sweep rates. The SFOAEs were extracted from the ear canal responses evoked with SSS in normally hearing subject s039(left ear). The stimulus parameters are $L_p=30$ dB SPL, $L_s=50$ dB SPL. The solid lines with different colors and the dotted lines with different colors, respectively, depict SFOAEs and NF extracted by the SSS technique.

SFOAEs in time domain and frequency domain for s040

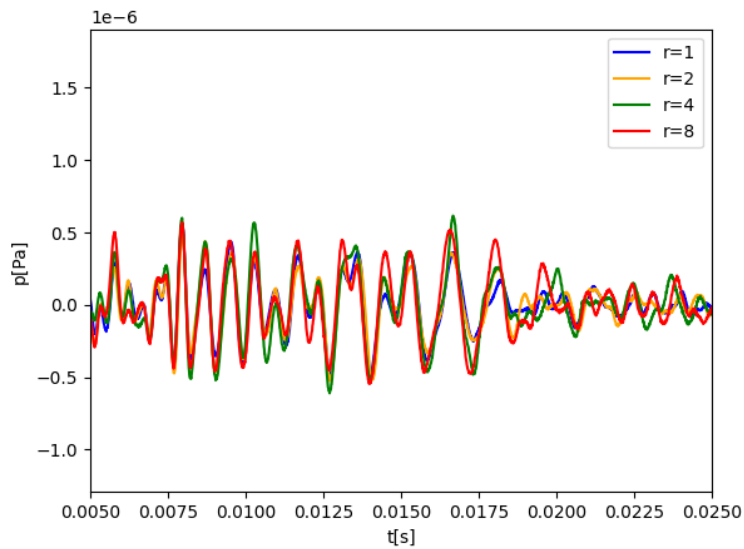


FIG.15. The "virtual" impulse responses showing SFOAEs in the time domain for different sweep rates for subject s040(left ear).

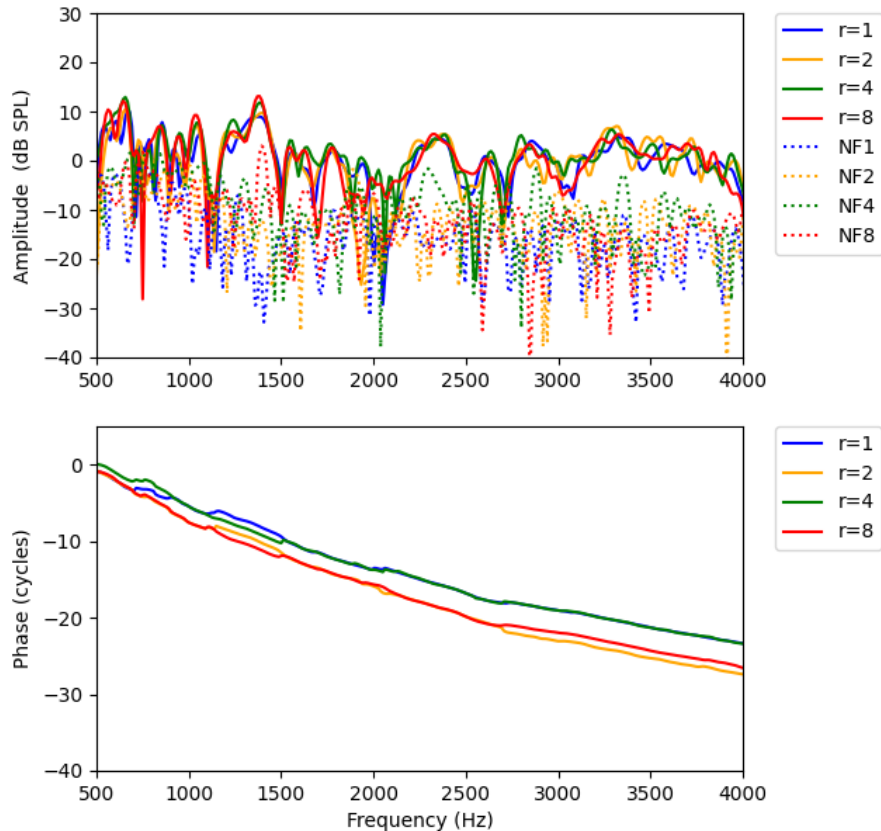


FIG.16. Amplitude and phase of SFOAEs for different sweep rates. The SFOAEs were extracted from the ear canal responses evoked with SSS in normally hearing subject s040(left ear). The stimulus parameters are $L_p=45$ dB SPL, $L_s=60$ dB SPL. The solid lines with different colors and the dotted lines with different colors, respectively, depict SFOAEs and NF extracted by the SSS technique.

SFOAEs in the time domain:

The above figure of these two groups shows the “virtual” impulse responses for different sweep rates of SFOAEs.

When we compare the curves corresponding to different sweep rates, it's noticeable that the amplitudes of the oscillations change. Higher sweep rates typically result in more rapid changes in amplitude over the same time period, which can lead to more tightly packed oscillations in the response graph.

SFOAEs in the frequency domain:

These graphs appear to display data related to SFOAEs measured at different sweep rates across a frequency spectrum, shown in both amplitude and phase components.

The consistency in the patterns of amplitude decline and phase shift across the different conditions suggests that the cochlear response characteristics remain stable across different sweep rates, and the variations seen are likely due to the SFOAEs' dependence on the stimulus frequency. From an analytical standpoint, the small variations in amplitude and phase across sweep rates might offer insights into the non-linear and frequency-dependent properties of the cochlea, particularly how it responds to different

rates of frequency change (sweep rates). The data could be used to understand the temporal dynamics of SFOAE generation and propagation within the ear.

The similarities in the overall shape of the curves (FIG.13, FIG.14, FIG.15 and FIG.16) suggest a consistent response amplitude with sweep rates from $r = 1$ oct/second to $r = 8$ oct/second. We can conclude that up to 8 oct/second, the SSS technique is usable to extract the SFOAE using the suppression method.

6. Conclusion

In our research, we aimed to integrate the SSS technique with traditional SFOAEs measurement methods to extract SFOAEs. The experiments conducted in exploring the effects of different stimulus intensities and sweep sine rates on SFOAEs. We can conclude that the SSS technique can be used with the suppression method to extract SFOAEs for various stimulus intensities for the sweep rate of 1 oct/sec with a modified, interleaved suppression paradigm. Upon exploring the effect of sweep rate on SFOAEs, we observed high consistency in SFOAEs across different sweep rates up to 8 oct/sec, underscoring the stability of SFOAEs against variations in the sweep rate under a constant stimulus intensity.

However, our research also raised certain queries and points for further discussion. For instance, under the investigation of stimulus intensity effects, an ideal suppression paradigm should not exhibit visible suppressor responses in the virtual impulse responses. Yet, the amplitude of suppressor responses at $L_s = 65$ dB SPL were significantly higher than those at $L_s = 50$ dB SPL. We hypothesize that this could indicate the activation of the middle ear muscle reflex at greater suppression intensities, potentially impeding the modified, interleaved suppression paradigm's ability to cancel out the suppressor response. Fortunately, our findings suggest that these residual suppressor responses are relatively minor and do not substantially impact the SFOAEs. On the contrary, we believe that our finding implies another advantage of the SSS technique, the presence of suppressor response may indicate an "issue" during the measurement, e.g. middle ear muscle reflex. So, the experimenter has a potentially important information usable for data interpretation.

Overall, the results pertaining to the two explored factors affecting SFOAEs are deemed objective and acceptable. Thus, we conclude that our approach of combining the SSS technique with traditional SFOAE measurement techniques for the extraction of SFOAEs is possible.

7. References

- [1]. Douglas H. Keefe, Kim S. Schairer, John C. Ellison, "Use of stimulus-frequency otoacoustic emissions to investigate efferent and cochlear contributions to temporal overshoot.", *J. Acoust. Soc. Am.* 2009 Mar; 125(3): 1595–1604. Available online: <https://doi.org/10.1121/1.3068443>
- [2]. Karolina K. Charaziak, Christopher A. Shera, "Reflection-Source Emissions Evoked with Clicks and Frequency Sweeps: Comparisons Across Levels.", *J Assoc Res Otolaryngol.* 2021 Dec; 22(6):641-658. Available online: <https://doi.org/10.1007/s10162-021-00813-3>
- [3]. Christopher A. Shera, John J. Guinan, Jr., "Stimulus-frequency-emission group delay: A test of coherent reflection filtering and a window on cochlear tuning.", *J. Acoust. Soc. Am.* 2003 May; 113, 2762–2772. Available online: <https://doi.org/10.1121/1.1557211>
- [4]. Stephen T. Neely, Tiffany A. Johnson, Michael P. Gorga, "Distortion-product otoacoustic emission measured with continuously varying stimulus level.", *J Acoust Soc Am.* 2005 Mar; 117(3 Pt 1): 1248–1259. Available online: <https://doi.org/10.1121/1.1853253>
- [5]. Carolina Abdala, Radha Kalluri, "Towards a joint reflection-distortion otoacoustic emission profile: Results in normal and impaired ears.", *J. Acoust. Soc. Am.* 2017; 142, 812–824. Available online: <https://doi.org/10.1121/1.4996859>
- [6]. Samantha Stiepan, Christopher A. Shera, Carolina Abdala, "Characterizing a Joint Reflection-Distortion OAE Profile in Humans with Endolymphatic Hydrops.", *Ear and Hearing*, 2023; 44(6): p 1437-1450. Available online: <http://doi.org/10.1097/AUD.0000000000001387>
- [7]. Radha Kalluri, Christopher A. Shera, "Comparing stimulus-frequency otoacoustic emissions measured by compression, suppression, and spectral smoothing.", *J. Acoust. Soc. Am.* 2007; 122, 3562–3575. Available online: <https://doi.org/10.1121/1.2793604>
- [8]. Antonin Novak, Pierrick Lotton, Laurent Simon, "Synchronized Swept-Sine: Theory, Application and Implementation.", October 2015; *JAES* Volume 63 Issue 10 pp. 786–798. Available online: <https://hal.science/hal-02504321/document>
- [9]. Václav Vencovský, Antonin Novak, Ondřej Klimeš, Petr Honzík, Aleš Vetešník, "Distortion-product otoacoustic emissions measured using synchronized swept-sines.", *J. Acoust. Soc. Am.* 2023; 153, 2586. Available online: <https://doi.org/10.1121/10.0017976>
- [10]. Christopher A. Shera, John J. Guinan, Jr, "Evoked otoacoustic emissions arise by two fundamentally different mechanisms: A taxonomy for mammalian OAEs.", *J. Acoust. Soc. Am.* 1999; 105, 782–798. Available online: <https://doi.org/10.1121/1.426948>

- [11]. Glenis R. Long, Carrick L, Talmadge, Jungmee Lee, "Measuring distortion product otoacoustic emissions using continuously sweeping primaries.", J. Acoust. Soc. Am. 2008; 124, 1613–1626. Available online:
<https://doi.org/10.1121/1.2949505>
- [12]. Yong-Sun Choi, Soo-Young Lee, Kourosh Parham, Stephen T. Neely, Duck O. Kim, "Stimulus-frequency otoacoustic emission: Measurements in humans and simulations with an active cochlear model.", J. Acoust. Soc. Am. 2008; 123, 2651–2669. Available online:
<https://doi.org/10.1121/1.2902184>
- [13]. The picture of an Etymotic ER 10C probe. Taken from the online website:
https://scitechkorea.com/bio/physiology_auditory_1page_etymotic_er-10c.html
- [14]. The sound device (connected) python library is available online:
<https://github.com/vencov/pySFOAE>